NHE3 Activity Is Dependent on Direct Phosphoinositide Binding at the N Terminus of Its Intracellular Cytosolic Region*[S]

Sachin Mohan[‡], Chung Ming Tse[‡], Sandra B. Gabelli[§], Rafiquel Sarker[‡], Boyoung Cha[‡], Kamau Fahie[§], Mythili Nadella[§], Nicholas C. Zachos[‡], Becky Tu-Sekine[¶], Daniel Raben[¶], L. Mario Amzel[§], and Mark Donowitz[‡1]

From the ‡Departments of Physiology and Medicine, Gastroenterology Division, and the Departments of §Biophysics and Biophysical Chemistry and ¶Biological Chemistry, The Johns Hopkins University School of Medicine, Baltimore, Maryland 21205

The small intestinal BB Na^+/H^+ antiporter NHE3 accounts for the majority of intestinal sodium and water absorption. It is highly regulated with both postprandial inhibition and stimulation sequentially occurring. Phosphatidylinositide 4,5-bisphosphate ($PI(4,5)P_2$) and phosphatidylinositide 3,4,5-trisphosphate ($PI(3,4,5)P_3$) binding is involved with regulation of multiple transporters. We tested the hypothesis that phosphoinositides bind NHE3 under basal conditions and are necessary for its acute regulation. His_6 proteins were made from the NHE3 C-terminal region divided into four parts as follows: F1 (amino acids 475–589), F2 (amino acids 590–667), F3 (amino acids 668–747), and F4 (amino acids 748–832) and purified by a nickel column. Mutations were made in the F1 region of NHE3 and cloned in pet30a and pcDNA3.1 vectors. $PI(4,5)P_2$ and $PI(3,4,5)P_3$ bound only to the NHE3 F1 fusion protein (amino acids 475–589) on liposomal pulldown assays. Mutations were made in the putative lipid binding region of the F1 domain and studied for alterations in lipid binding and Na^+/H^+ exchange as follows: Y501A/R503A/K505A; F509A/R511A/R512A; R511L/R512L; R520/FR527F; and R551L/R552L. Our results indicate the following. 1) The F1 domain of the NHE3 C terminus has phosphoinositide binding regions. 2) Mutations of these regions alter $PI(4,5)P_2$ and $PI(3,4,5)P_3$ binding and basal NHE3 activity. 3) The magnitude of serum stimulation of NHE3 correlates with $PI(4,5)P_2$ and $PI(3,4,5)P_3$ binding of NHE3. 4) Wortmannin inhibition of PI3K did not correlate with $PI(4,5)P_2$ or $PI(3,4,5)P_3$ binding of NHE3. Two functionally distinct phosphoinositide binding regions (Tyr^{501}–Arg^{512} and Arg^{520}–Arg^{552}) are present in the NHE3 F1 domain; both regions are important for serum stimulation, but they display differences in phosphoinositide binding, and the latter but not the former alters NHE3 surface expression.

Many transport proteins, including pumps, channels, and transporters, are regulated by phosphoinositides. This rapidly

expanding list includes voltage-gated K^+ channels, inwardly rectifying K^+ channels, and members of the TRP channel family, ENaC, NHE1, and NBCe1 (1–8). This regulation has been explained on the basis of two contrasting mechanisms. (i) There is direct phosphoinositide interaction with specific amino acids in the transport protein, explained either on the basis of charge (8–13) or presence of canonical lipid binding domains such as pleckstrin homology domains (1, 8, 14). Common to these direct interaction studies has been the demonstration that mutagenesis of specific amino acids leads to changes in molecular interactions with phosphoinositides that lead to subsequent changes in physiologic channel or transporter activity. (ii) An indirect mechanism involves an additional intermediate, either protein or lipids, that binds via a phosphoinositide-dependent mechanism (5, 11).

Sodium/hydrogen exchangers (SLC9a family) are ubiquitous transporters serving many functions in the cell, including regulation of intracellular pH, cell volume, and sodium absorption (15, 16). Grinstein and co-workers (17) have demonstrated that NHE1, the ubiquitous member of the sodium hydrogen exchanger gene family, is regulated by $PI(4,5)P_2$, which binds to its C terminus. Using a unique whole cell patch pipette technique, Fuster et al. (18) showed that NHE3 is rapidly stimulated in opossum kidney cells by intracellular application of $PI(3,4,5)P_3$.[2] However, the mechanism of this stimulation is unknown. We hypothesized that the epithelial brush border Na^+/H^+ antiporter NHE3 binds phosphoinositides based on the recognition that gene families have similar structural/functional organization (19). The aim of this study was to understand the mechanism of NHE3 regulation by phosphoinositides by the following: (i) investigating whether NHE3 can directly bind phosphoinositides; (ii) identifying regions and amino acids that are necessary for this interaction; and (iii) studying the physiologic relevance of this interaction.

EXPERIMENTAL PROCEDURES

Materials—Lipids, phosphatidylcholine, phosphatidylethanolamine, phosphatidylserine, $PI(3,4,5)P_3$, and $PI(4,5)P_2$ were from Avanti Polar Lipids. QuikChange site-directed mutagenesis kit was from Stratagene (La Jolla, CA). EZ-link sulfo-NHS-

A

CHP   LBG   Ez

```
NHE3_RAT      471 KLNEKLHGRAFDHILSAIEDISGQIGHNYLRDKWSNFDRKFLSKVLMRRSAQKSRDRILN 530
NHE3_OPOSSUM  479 KLNEKLHGRAFDHILSAIEDISGQIGHNYLRDKWSNFDRKVLSKLLMRRSAQKSRDRILN 538
NHE3_HUMAN    474 RLNEKLHGRAFDHILSAIEDISGQIGHNYLRDKWSHFDRKFLSRVLMRRSAQKSRDRILN 533
NHE3_RABBIT   473 KLNEKLHGRAFDHILSAIEDISGQIGHNYLRDKWANFDRRFLSKLLMRQSAQKSRDRILN 532
                  :********************************:::*:.**::.**:**********
```

```
NHE3_RAT      531 VFHELNLKDAISYVAEGERRGSLAFIRSPSTDMMVNVDFSTPRPSTVEASVSYFLRENVS 590
NHE3_OPOSSUM  539 VFHELNLKDAISYVAEGERRGSLAFIRSPSTDNIVNVDFSTPRPSTVEASVSYLLRENVS 598
NHE3_HUMAN    534 VFHELNLKDAISYVAEGERRGSLAFIRSPSTDNVVNVDF-TPRPSTVEASVSYLLRENVS 592
NHE3_RABBIT   533 VFHELNLKDAISYVTEGERRGSLAFIRSPSTDMMVNVDFSTPRPSTVEASVSYLLRESAS 592
                  **************:********************* ***.*********:***..*
```

〰〰〰   CHP binding area

▬▬   Positively charged amino acid clusters. Boxes indicate amino acids which were mutated in the current study.

⌐⌐   Underlined is NHE3 positive amino acid cluster which is homologus to identified NHE3 PI(4,5)P$_2$ binding domain.

LBG   Lipid Binding Group as predicted by Scansite with critical F indicated in bold box.

Ez   Direct Ezrin binding area

B

```
          I
NHE1RAT   477 HFPMCDLFLTAIITVIFFTVFVQGMTIRPLVDLLAVKKKQETKRSINEEIHTQFLDHLLT 536
NHE1HUMAN 473 HFPMCDLFLTAIITVIFFTVFVQGMTIRPLVDLLAVKKKQETKRSINEEIHTQFLDHLLT 532
NHE3RABBIT 429 KVKEKNLFVSTTIIVVFFTVIFQGLTIKPLVQWLKVKRSEHRPEKLNEKLHGRAFDHILS 488
NHE3RAT   427 KVKEKNLFVSTTLIVVFFTVIFQGLTIKPLVQWLKVKRSEQRPEKLNEKLHGRAFDHILS 486
              :.     :**::: : *:****.:.**.:**:*  * **:.. : .:**::* : :**:*
```

```
              II
NHE1RAT   537 GIEDICGHYGHHHWKDKLNRFNKKYVKKCLIAGERSKE-PQLIAFYHKMEMKQAIELVES 595
NHE1HUMAN 533 GIEDICGHYGHHHWKDKLNRFNKKYVKKCLIAGERSKE-PQLIAFYHKMEMKQAIELVES 591
NHE3RABBIT 489 AIEDISGQIGHNYLRDKWANFDRRFLSKLLMRQSAQKSRDRILNVFHELNLKDAISYVTE 548
NHE3RAT   487 AIEDISGQIGHNYLRDKWSNFDRKFLSKVLMRRSAQKSRDRILNVFHELNLKDAISYVAE 546
              .****.*: **::*:   :** .*:::::*: *:   .*.  ::: .:*::::*:**. *.
```

```
NHE1RAT   596 GGMG------KIPSAVTVSMQNIHPKSAASERILPALSKD-------------------- 630
NHE1HUMAN 592 GGMG------KIPSAVTVSMQNIHPKSLPSERILPALSKD-------------------- 626
NHE3RABBIT 549 GERRGSLAFIRSPSTDNMVNVDFSTPRPSTVEASVSYLLRESASAVCLDMQSLEQRRRSV 608
NHE3RAT   547 GERRGSLAFIRSPSTDMMVNVDFSTPRPSTVEASVSYFLRENVSAVCLDMQSLEQRRRSI 606
              *        : **:: .  *:::   *::. .  *  :::. : :::
```

▬▬▬▬   PI(4,5)P$_2$ binding motifs I,II in NHE1 (O. Aharanovitz et. al. 1999)

▭▭▭▭   Scansite prediction for lipid binding group in NHE3

▭▭▭▭   Lipid interaction domain in NHE1 (Wakabayashi et. al. 2010)

▭▭▭▭   Lipid binding area in NHE3 based on current study

FIGURE 1. Bioinformatic analysis of NHE3. *A*, NHE3 F1 region (amino acids 475–589) is conserved across species and shown in the figure is the Scansite prediction for the presence of the lipid binding group (*LBG*) in this area. Phe[509] is predicted to be necessary for lipid binding in Scansite analysis and is shown here in a *bold box*. Clusters of positively charged and aromatic amino acids are shown as *bars*, with mutated residues shown in *boxes*. Calcineurin homologous protein (*CHP*) binding area is shown as a *jagged bar*. Direct Ezrin binding area is shown as *Ez*. *B*, alignment of NHE1 rat, NHE1 human, NHE3 rabbit, and NHE3 rat. Motifs I and II indicate clusters of positively charged amino acids, previously shown to be important for phosphoinositides binding in NHE1 (17). Lipid interaction domain of NHE1 is shown in *red*. Lipid binding group (*LBG*) in NHE3 as predicted by Scansite is shown as a *green bar*. Lipid binding region in NHE3 as identified by this study is shown in *green*. * indicates identical amino acids; : indicates conserved amino acids; and . indicates semiconserved amino acids.

Construction of Expression Vectors for NHE3 C-terminal His$_6$ Fusion Proteins and NHE3 C-terminal Point Mutations—Four His$_6$-tagged cDNAs together spanning nearly the entire rabbit NHE3 C terminus were engineered by PCR to encode F1(amino acids 475–589), F2 (amino acids 590–667), F3 (amino acids 668–747), and F4 (amino acids 748–832). Fragments were ligated into pET 30a vector (Novagen) with N-terminal His$_6$ tag using HindIII and EcoRI restriction sites. A 2-amino acid linker (LL) was placed at the C terminus, and a stop codon was inserted at the 3′ end for all inserts just after the linker region. Point mutations in full-length NHE3 were prepared using QuikChange site-directed mutagenesis kit according to the manufacturer's protocol (Table 1). All the cDNAs were fully sequenced to ensure proper sequence, orientation, and reading frame.

Cell Culture and cDNA Transfection of NHE3 C-terminal Point Mutations—The cDNAs of wild type (WT) rabbit (HA) NHE3 and point mutants Y501A/R503A/K505A, F509A/R511A/R512A, R511L/R512L, and R551L/R552L in pcDNA3.1/G418 (Invitrogen) consisting of an N-terminal triple HA tag, as described previously (20), were transfected into plasma membrane Na$^+$/H$^+$ exchanger-deficient PS120 fibroblasts (stably expressing NHERF2 with a hygromycin-resistant selectable marker) at 70% confluence, using ~10 µl of Lipofectamine 2000 (Invitrogen) according to the manufacturer's protocol. Similarly, point mutation R520F/R527F with a C-terminal VSV-G epitope tag in pcDNA3.1/hygromycin was transfected into PS120 fibroblasts stably expressing NHERF2 (21). Cells stably transfected with NHE3 (NHE3 wild type and mutants) were selected by an H$^+$ selection procedure consisting of exposure to 50 mM NH$_4$Cl/saline solution for 1 h, followed by an isotonic 2 mM Na$^+$ solution for 1 h, as described previously (22). Surviving cells were placed in normal culture medium (Dulbecco's modified Eagle's medium with 4.5 g/liter glucose, 584 mg/ml L-glutamine, 110 mg/ml sodium pyruvate, and 10% FBS) with hygromycin and G418 to maintain selection pressure and allowed to reach 30–50% confluence. The H$^+$ selection process was initially repeated every 2–3 days

SS-biotin was from Thermo Scientific (Rockford, IL). Nigericin and 2′,7′-bis(2-carboxyethyl)-5(6)-carboxyfluorescein were from Invitrogen. DNA primers were from Operon Biotechnologies (Huntsville, AL). Unless specified, all other chemicals and materials were from Sigma.

Antibodies—Monoclonal mouse antibodies to the hemagglutinin (HA) epitope (MMS 101-R) were from Covance Research Products (Princeton, NJ). Monoclonal mouse anti-polyhistidine antibodies (H1029) and monoclonal mouse anti-VSV-glycoprotein antibodies (A1970) were purchased from Sigma.
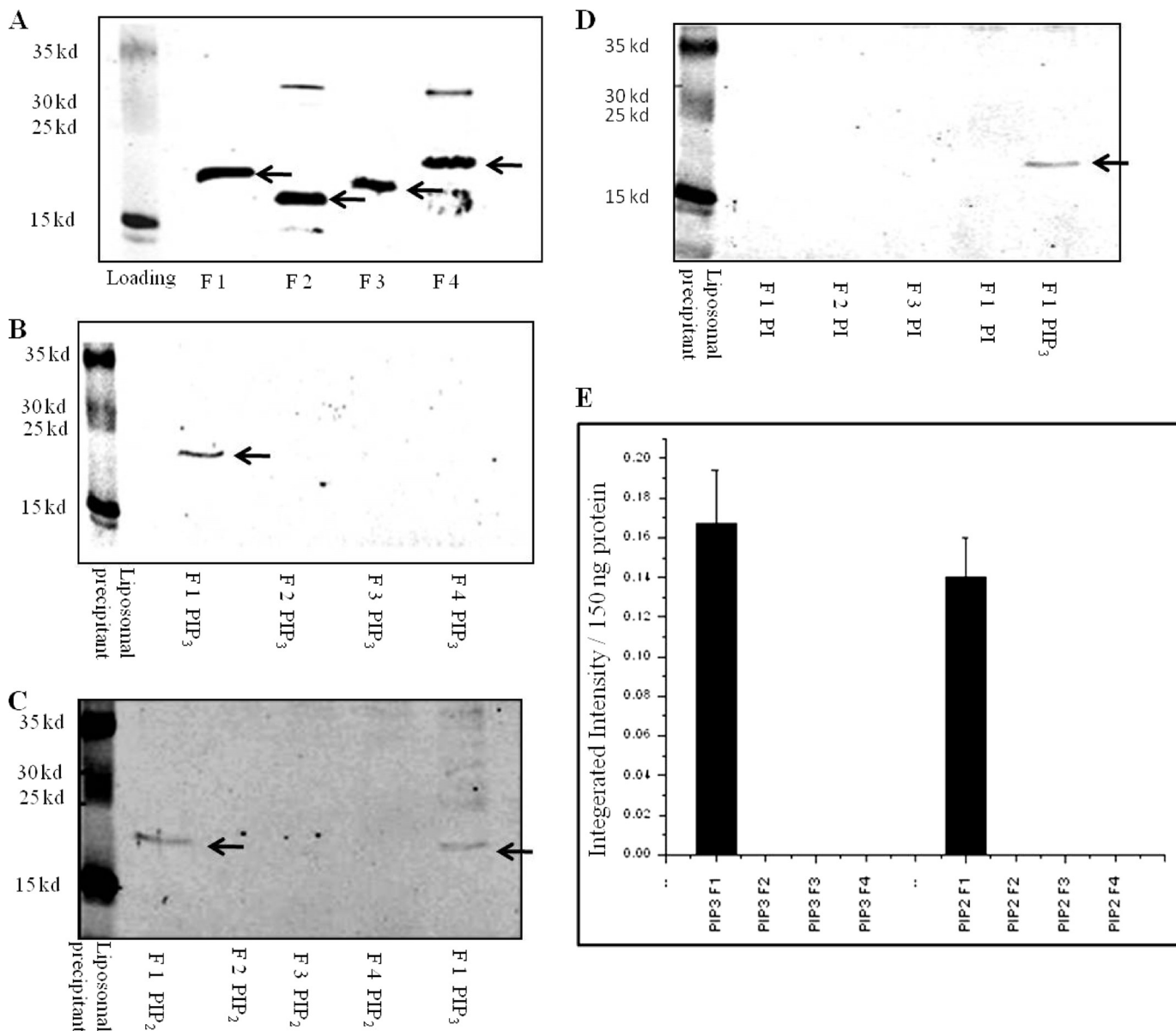
FIGURE 2. **F1 region of rabbit NHE3 (amino acids 475–589) binds to liposomes containing PI(3,4,5)P$_3$ and PI(4,5)P$_2$ but not PI.** *A,* Western blot showing 150 ng of His$_6$ NHE3 C-terminal fusion proteins F1, F2, F3, and F4. These represent input for all experiments. *Arrows* indicate major bands detected by anti-His$_6$ antibody, 1:5000. *B,* only F1 but not F2, F3, or F4 bind with PI(3,4,5)P$_3$ in liposomal pulldown assays. Representative Western blots are shown that were repeated three times with similar results. 150 ng of each NHE3 fusion protein was used in liposomes consisting of 30 mol % phosphatidylcholine, 17 mol % phosphatidylserine, 20 mol % phosphatidylethanolamine, 24.75 mol % phosphatidylinositol, and 8.25 mol % PI(3,4,5)P$_3$. *C,* only F1 but not F2, F3, or F4 binds with PI(4,5)P$_2$. Liposomes as in Fig. 1*B,* except 8.25 mol % PI(4,5)P$_2$, were used instead of PI(3,4,5)P$_3$. A representative Western blot is shown, which was repeated four times with similar results. *Right lane* is positive control showing F1 fragment binding with PI(3,4,5)P$_3$ liposomes. *D,* no binding to PI. 150 ng of each NHE3 fusion protein was used with liposomes as in *B* and *C* but with 33 mol % phosphatidylinositol. A PI(3,4,5)P$_3$ liposomal pulldown with F1 is shown in the *right lane* as a positive control. A representative Western blot is shown, which was repeated three times with similar results. *E,* quantification for binding from *B* and *C* was done by measuring integrated signal intensity of bands by Odyssey system (LI-COR, Lincoln, NE) normalized to 150 ng of fusion protein. Integrated intensity of bands shown as means $\pm$ S.E. for PI(3,4,5)P$_3$, $n = 3$, and PI(4,5)P$_2$, $n = 4$, is plotted on the *y* axis. Only the F1 fragment bound PI(3,4,5)P$_3$ and PI(4,5)P$_2$. *Arrows* in Fig. 2, *B–D* indicate F1 fragment in liposomal pulldowns.

until more than 50% of the cells survived and was then repeated weekly thereafter.

Expression and Purification of Escherichia coli Fusion Proteins—Rosetta 2 (DHE-3) cells grown in Luria broth (LB) medium were used to express His$_6$-tagged fusion proteins using 1 mM isopropyl 1-thio-β-D-galactopyranoside for induction. Crude cell extracts were prepared from culture pellets by breaking the cells in a microfluidizer. Lysates were loaded on columns packed with a Ni^{2+}-nitrilotriacetic acid resin. The col-

umn was washed five times with 50 mM Tris, pH 7.4, and 300 mM NaCl and eluted in 50 mM Tris, pH 7.4, 300 mM NaCl and 250 mM imidazole (protocol modified from Qiagen, Valencia, CA). The proteins were subjected to SDS-PAGE and stained with Coomassie Blue demonstrating a single predominant band for each protein (supplemental Fig. 2).

In Vitro Liposomal Binding Assays—PI(4,5)P$_2$, PI(3,4,5)P$_3$, or PI lipid vesicles were prepared with 30 mol % phosphatidylcholine, 17 mol % phosphatidylserine, 20 mol % phosphatidyleth-

anolamine, 24.75 mol % phosphatidylinositol (PI) and 8.25 mol % PI(3,4,5)P$_3$, PI(4,5)P$_2$ or additional PI (in control experiments). Vesicles with serial dilutions of PI(4,5)P$_2$, PI(3,4,5)P$_3$, or PI were prepared by altering molar concentrations of PI with respect to PI(4,5)P$_2$ or PI(3,4,5)P$_3$, keeping the total molar concentration at 100 mol %. The lipids were dried in a speed vacuum and rehydrated using bath sonication in 250 μl of 0.2 M sucrose, 20 mM KCl, 20 mM HEPES, pH 7.4, 0.01% sodium azide. 150 of ng of test proteins (F1, F2, F3, F4, and point mutations) were mixed with 100 μl of PI(3,4,5)P$_3$, PI(4,5)P$_2$, or PI vesicles in 900 μl of liposomal reaction buffer (containing 0.12 M NaCl, 1 mM EGTA, 0.2 mM CaCl$_2$, 1 mM MgCl$_2$, 5 mM KCl, 20 mM HEPES, pH 7.4, 1 mg/ml BSA, and 0.75 mM fresh DTT) and incubated for 15 min at 37 °C. The 1000-μl mixture was then ultracentrifuged at 100,000 $\times$ *g* for 45 min in a Beckman Ti70.1 rotor. The supernatant was removed by fine tip vacuum suction, and the pellet thus obtained was resuspended in NuPAGE LDS sample buffer (Invitrogen) preheated at 60 °C and bath-sonicated for 10 min at room temperature. 35 μl of sample was separated on 14% SDS-PAGE and transferred onto nitrocellulose for immunoblot analysis.

Immunoblot Analysis—The membranes were blocked with 5% nonfat dry milk in phosphate-buffered saline (PBS) (10 mM potassium phosphate buffer, pH 7.4, and 0.15 M NaCl) for 1 h. Blots were then incubated with primary antibodies (where indicated: anti-His (1:5000); anti-HA (1:1000); anti VSVG (1:100)) in 5% milk/PBS for 1 h at room temperature and then washed with 0.05% Tween/PBS three times for 10 min each. The blots were incubated with fluorescently labeled secondary antibody goat anti-mouse IRDye 800 at 1:15,000 (Rockland Immunochemicals, Gilbertsville, PA) for 1 h. Finally, blots were washed three times for 10 min each with 0.05% Tween/PBS, and bands were visualized by the Odyssey system (LI-COR, Lincoln, NE).

Measurement of Na$^+$/H$^+$ Exchange Activity—The transfected PS120 cells were grown to a confluence of ~70% on glass coverslips and then placed in serum-free medium for 4–5 h to arrest cell division. The Na$^+$/H$^+$ exchanger activity of these cells was measured fluorometrically by using the intracellular pH-sensitive dye 2′,7′-bis(2-carboxyethyl)-5(6)-carboxyfluorescein acetoxymethyl ester (21). The experiments were performed under basal, stimulated (10% dialyzed serum), and inhibited conditions (100 nM wortmannin). To study the effect of serum, PS120 cells were incubated with NH$_4$Cl medium with 10% serum for 20 min at 37 °C. This was followed by sequential perfusion with tetramethylammonium and Na$^+$ media containing 10% serum as described previously (22). Study of the wortmannin effect was by adding 100 nM wortmannin to NH$_4$Cl medium and incubating for 45 min at 37 °C followed by perfusion with tetramethylammonium and Na$^+$ media. Na$^+$/H$^+$ exchange rates (H$^+$ efflux) were calculated as the product of buffering capacity at each pH$_i$ and Na$^+$-dependent change in pH$_i$ and were analyzed using data analysis software Origin (Microcal), by which data are fit to a general allosteric model as described by the Hill equation. In all experiments, V_{max} and K' (H$^+$)$_i$ values were calculated. Means $\pm$ S.E. were calculated from kinetic parameters from at least five different experiments for each condition.
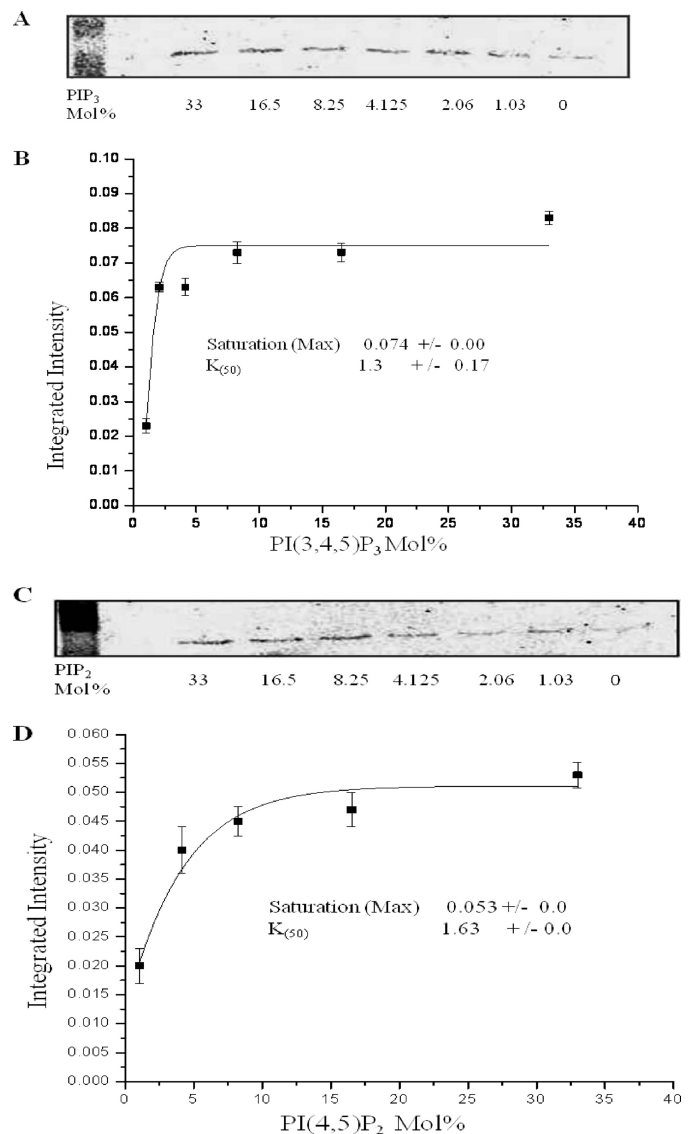
FIGURE 3. **NHE3-F1 fusion protein binds to liposomes containing PI(3,4,5)P$_3$ and PI(4,5)P$_2$ in a saturable manner.** *A,* liposomal pulldowns assays performed with 150 ng of F1 protein and liposomes containing varied amounts of PI(3,4,5)P$_3$. The makeup of the liposomes was set at 100 mol % by replacing mol % of PI(3,4,5)P$_3$ by the same mol % PI. His$_6$-tagged NHE3 F1 was identified by Western blot analysis of the pulldown by anti-His$_6$ antibody, and the intensity of bands was quantified by Odyssey system (LI-COR). *B,* binding curve based on intensity values (*y* axis) *versus* PI(3,4,5)P$_3$ in mol % (*x* axis). Background intensity due to F1 protein binding in absence of PI(3,4,5)P$_3$ was subtracted from all data points in calculating kinetics of binding. All experiments were done three times, and the *curve* representing means $\pm$ S.E. calculated from data points of three different experiments is shown. Saturation (max) and K_{50} were calculated using Origin software. *C,* liposomal pulldowns done with 150 ng of F1 protein and liposomes containing varied amounts of PI(4,5)P$_2$; PI(4,5)P$_2$ was replaced by the same mol % PI in PI(4,5)P$_2$ liposomes. Intensity of bands was quantified by Odyssey system (LI-COR). *D,* binding curve based on intensity values (*y* axis) *versus* PI(4,5)P$_2$ in mol % (*x* axis). Background intensity due to F1 protein binding in the absence of PI(4,5)P$_2$ was subtracted from all data points in calculating kinetics of binding. All experiments were done three times, and the binding curve representing means $\pm$ S.E. calculated from data point of three different experiments is shown. Saturation (max) and K_{50} values (mol %) were calculated using Origin software.

Cell Surface Biotinylation—The transfected PS120 cells were grown to 70–80% confluence in 10-cm Petri dishes. The cells were then serum-starved for 4–5 h. Cells were washed with ice-cold phosphate-buffered saline three times (150 mM NaCl

NHE3 Activity and Direct Phosphoinositide Binding

Cell Type (PS120 / NHERF2)	Basal Activity uM/sec	Serum	Wort	% Surface	Total Expression (% of wt)	Molecule per surface	Relative Transport per Molecule	Binding to PIP$_2$	Binding to PIP$_3$
1. WT	818	↑ 75%	↓ 50%	6.3	100%	6.3	130	+++	+++
2. Y501A/R503A/K505A	297	NE	NE	5.1	44%	2.2	135	-	-
3. F509A / R511A / R512A	452	↑ 55%	↓ 68%	5.1	42%	2.1	215	-	-
4. R511L / R512L	76	↑160%	↓ 30%	1.3	13.5%	0.2	380	+++++	+++++
5. R520F / R527F	396	NE	↓ 50%	1.9	100%	1.9	208	+ +	+
6. R551L / R552L	263	NE	↓ 50%	2.8	86%	2.4	109	-	-
7. Y501A / R503A / K505A + F509A / R511A / R512A	277	NE	NE	4.7	28%	1.3	213	-	-

and 20 mM Na$_2$HPO$_4$, pH 7.4) and subsequently once in borate buffer (1 mM boric acid, 154 mM NaCl, 7.2 mM KCl, and 1.8 mM CaCl$_2$, pH 9.0). The surface labeling of NHE3 was done by incubating cells with 0.5 mg/ml sulfo-NHS-SS biotin (21) for 20 min and repeated once. Post-labeling, the cells were washed three times with quenching buffer (20 mM Tris, pH 7.4, and 120 mM NaCl) to scavenge the unreacted biotin. Cells were washed three times with ice-cold phosphate-buffered saline and solubilized with N$^+$ lysis buffer (60 mM HEPES, pH 7.4, 150 mM NaCl, 3 mM KCl, 5 mM Na$_3$EDTA, 3 mM EGTA, and 1% Triton X-100). The lysates were then incubated with streptavidin-agarose beads for 4 h. After precipitation of the streptavidin-agarose complex, the supernatant was recovered and called the intracellular fraction. The avidin-agarose beads were washed in N$^+$ buffer six times. For recovering the plasma membrane NHE3, the streptavidin-agarose beads were resuspended in loading buffer (5 mM Tris-HCl, pH 6.8, 1% SDS, 10% glycerol, and 1% 2-mercaptoethanol), boiled for 5 min at 70 °C, and separated on 10% SDS-PAGE. The size-fractionated gel was then transferred electrophoretically to nitrocellulose. After blocking for 1 h in 5% non-fat milk, the blots were probed with monoclonal anti-HA antibody. Western analysis and quantification of the surface fraction were performed using Odyssey software (LI-COR, Lincoln, NE), as described previously (23). As shown in Table 1, in our studies with WT and mutant NHE3, the total expression of mutations was normalized to the WT expression level, which was set at 100% in each experiment.

Statistical Analysis—All numerical data are expressed as means ± S.E., and Student's *t* tests were used to calculate significance of difference between experimental groups.

RESULTS

Identification of a Phosphoinositide-binding Site in NHE3 by Bioinformatic Analysis—We hypothesized that the NHE3 C-terminal regulatory domain binds phosphoinositides, and we performed a bioinformatics analysis of the amino acid composition of the NHE3 C terminus using Scansite. A region in the NHE3 C-terminal domain, consisting of amino acids 502–516, was predicted by Scansite to be a candidate for lipid binding. This was not predicted by several other bioinformatics programs. This was conserved across species of NHE3. This region (Fig. 1A) has an estimated isoelectric point of 10 and contains clusters of positively charged and aromatic amino acids. The bioinformatics programs PFAM, ProSite, and Smart data bases

did not identify any putative lipid binding domains in the NHE3 C terminus (specific searches for pleckstrin homology, Phox homology, FYVE (Fab-1, YGL023, Vps27, and EEA1), C1, C2, BAR (Bin, amphiphysin, Rvs), GLUE (GRAM-like ubiquitin-binding in EAP45), FERM (band 4.1, ezrin, radixin, moesin), CLAM (clathrin assembly lymphoid myeloid), and GRAM (glucosyltransferases, Rab-like GTPase activators, and myotubularins) domains were performed). This made it unlikely that such domains were involved in any NHE3-plasma membrane lipid interactions leaving the possibility of charge and hydrophobicity based interactions in the area predicted by Scansite. Therefore, as a first step we determined whether the NHE3 C terminus, including the amino acids predicted to bind lipids by Scansite (amino acids 502–516), bound $PI(4,5)P_2$ or $PI(3,4,5)P_3$.

N-terminal Part of the Intracellular Domain of NHE3 (Amino Acids 475–589) but Not Other Parts of the NHE3 C Terminus Bind $PI(4,5)P_2$ and $PI(3,4,5)P_3$—To experimentally test whether the NHE3 C terminus directly binds phosphoinositides and where that binding occurs, we used liposomal pulldown assays with 150 ng of NHE3 C-terminal His$_6$ fusion proteins ($\sim$10 nM) and artificial liposomes (Fig. 2A). The F1 fragment of the NHE3 C terminus (amino acids 475–589) bound to liposomes containing either $PI(3,4,5)P_3$ (Fig. 2B) or $PI(4,5)P_2$ (Fig. 2C). No binding to PI(4,5)P2 or PI(3,4,5)P3 occurred with 150 ng of C-terminal fragments of NHE3 F2 (amino acids 590–667), F3 (amino acids 668–747), or F4 (amino acids 748–832). Binding to F1 was saturable for $PI(3,4,5)P_3$ and $PI(4,5)P_2$. Both phosphoinositides had similar K_{50} values of 1.3 mol % for $PI(3,4,5)P_3$ and 1.6 mol % for $PI(4,5)P_2$ as shown in Fig. 3.

As a negative control, binding of the F1 fragment did not occur with liposomes with 33 mol % of phosphatidylinositol, an unphosphorylated phospholipid (Fig. 2D). Further studies explored how the F1
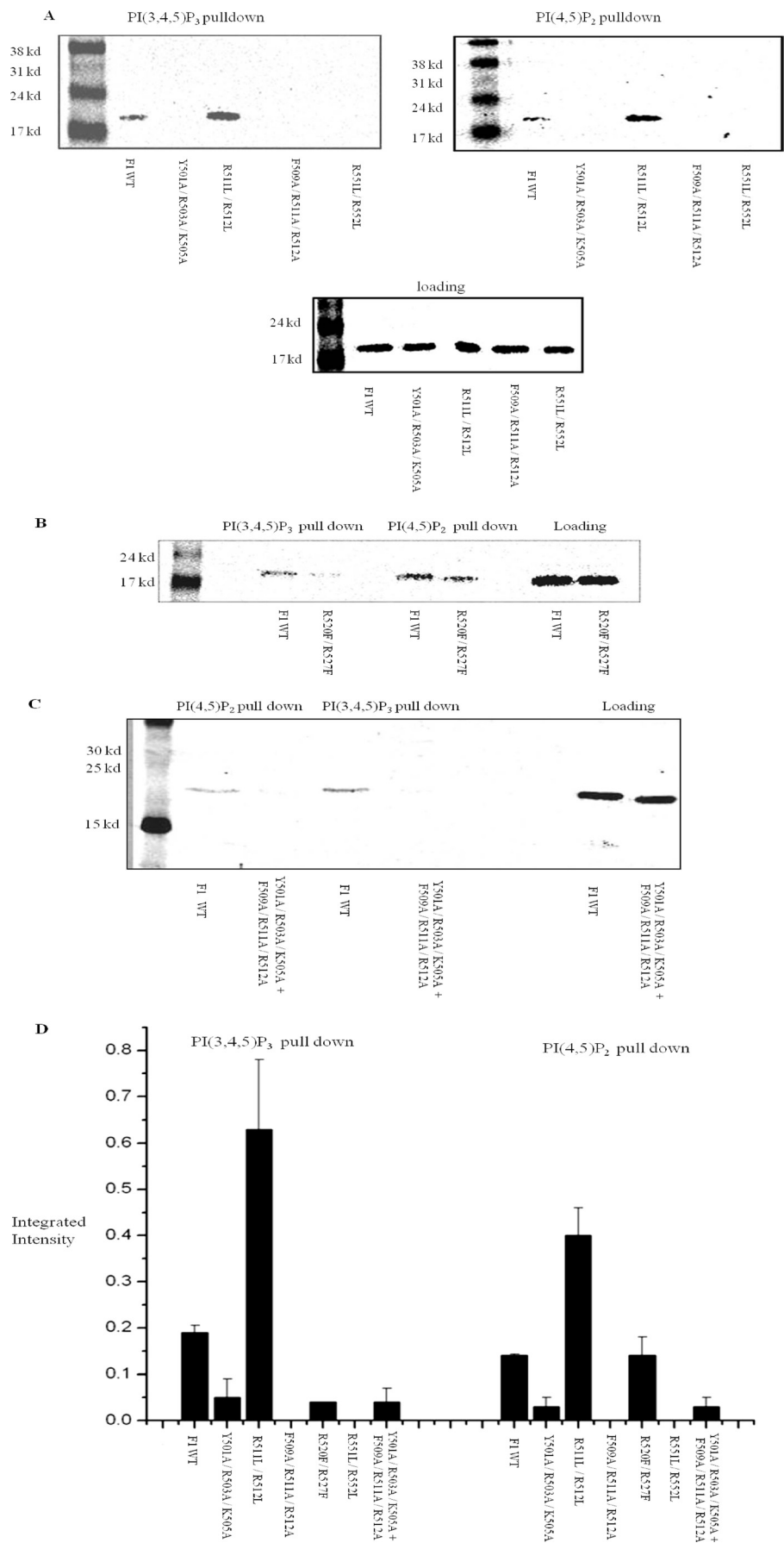
domain bound to $PI(3,4,5)P_3$ and $PI(4,5)P_2$ and the functional consequences of that binding.

Mutation of Positively Charged and Hydrophobic Amino Acids in the NHE3 C-terminal F1 Region Alters $PI(3,4,5)P_3$ and $PI(4,5)P_2$ Binding—Phosphoinositides bind to sites containing positively charged and aromatic amino acids (1). By sequence analysis, we identified four putative binding motifs in the F1 region of NHE3 (amino acids 475–589), which contain clusters of positive charges and were conserved across species of NHE3 (Fig. 1*A*). As shown in Fig. 1*A*, these clusters were located C-terminal to the putative calcineurin homologous protein binding area of NHE3, which we predicted by homology to the NHE1 calcineurin homologous protein-binding site, the structure of which had been solved (24, 25). One of these positively charged amino acid clusters (Arg^{520}/Arg^{527}) has previously been shown to be involved in the direct binding of the cytoskeletal linking protein ezrin to the NHE3 C terminus (21). A second motif ($Tyr^{501}/Arg^{503}/Lys^{505}$) is immediately adjacent to His^{499}, which had been shown by mutagenesis to be part of the NHE3 intracellular pH sensor (26).

To determine whether any of these conserved areas of clustered positively charged amino acids contributed to the interaction of NHE3 with $PI(3,4,5)P_3$ and/or $PI(4,5)P_2$, we individually mutated at least two positive charges in each cluster. In several instances, we also mutated an aromatic amino acid in the region. His_6 fusion proteins of the mutated F1 domains were studied for phosphoinositide binding, and the same mutations were made in full-length NHE3 and expressed in PS120/NHERF2 cells for Na^+/H^+ exchange activity measurements. Table 1 lists the mutations that were made in these domains with arginine or lysine being generally mutated to an alanine or leucine except for R520F/R527F, a mutation that had previously been shown to reduce direct ezrin binding to NHE3 (21).

Liposomal pulldown assays with purified mutant F1 domains confirmed binding of wild type NHE3 to liposomes containing $PI(3,4,5)P_3$ and $PI(4,5)P_2$. In contrast, the NHE3 F1 point mutants Y501A/R503A/K505A, F509A/R511A/R512A, R551L/R552L, and combination mutation Y501A/R503A/K505A + F509A/R511A/R512A showed loss of phosphoinositide binding. Mutation R520F/R527F displayed greater loss of $PI(3,4,5)P_3$ (68.1%) binding than $PI(4,5)P_2$ binding (23.3%). In contrast, the F1-R511L/R512L mutant exhibited increased binding to both $PI(3,4,5)P_3$- and $PI(4,5)P_2$-containing liposomes (Fig. 4, *A–D*).

Basal Transport and Serum Stimulation of NHE3 Activity but Not Wortmannin Inhibition of Basal Activity Directly Correlates with $PI(3,4,5)P_3$ and $PI(4,5)P_2$ Binding of NHE3—The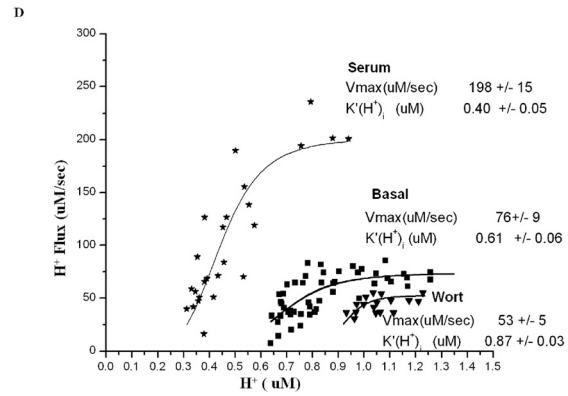 function of $PI(4,5)P_2$ and 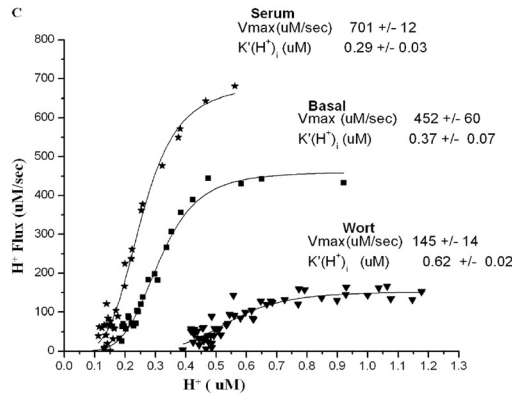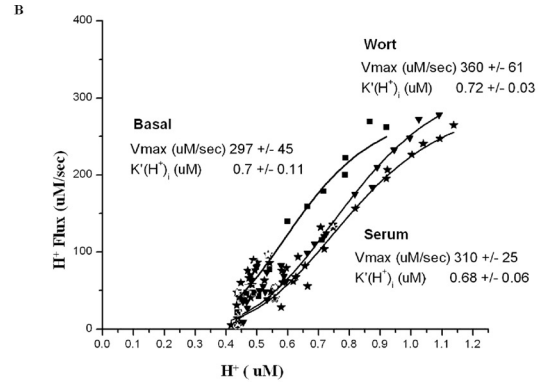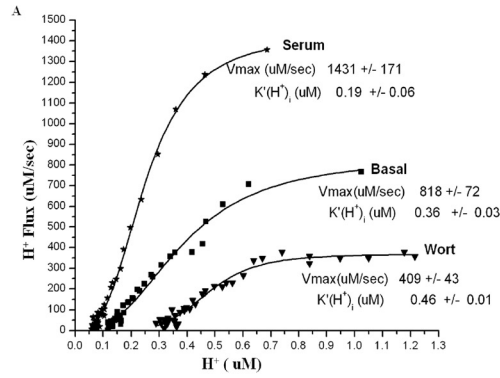$PI(3,4,5)P_3$ binding on NHE3 transport activity was studied in PS120/NHERF2 cells transfected with wild type NHE3 and full-length NHE3 mutated to contain the same point mutations listed in Table 1. Kinetic constants of WT NHE3 activity were compared with the mutants under basal, serum-stimulated, and wortmannin-inhibited conditions (Fig. 5, *A–H,* Table 1, and supplemental Table 1). All mutants with altered phosphoinositide binding displayed lower basal activity. This was true for both V_{max} and $K'(H^+)_i$. Those mutants with decreased phosphoinositide binding had decreased or absent serum stimulation of NHE3 activity. In contrast, the single mutant with increased $PI(3,4,5)P_3$ and $PI(4,5)P_2$ binding (R511L/R512L) had increased serum stimulation of NHE3 activity.

Under basal conditions, WT NHE3 (Fig. 5, *A* and *H*, Table 1, and supplemental Table 1) had transport activity of 818 ± 72 $\mu M/s$ (V_{max}) and $K'(H^+)_i$ of 0.36 ± 0.03 μM. NHE3 responded to serum with the following: (i) 75% increase in V_{max}, 1431 ± 171 $\mu M/s$, $p < 0.05$ and (ii) $K'(H^+)_i$ change to 0.19 ± 0.06 μM, $p < 0.05$ (increased sensitivity to H^+). Wortmannin-inhibited basal NHE3 activity was as follows: 50% inhibition of V_{max}, 409 ± 43 $\mu M/s$, $p < 0.005$, and (ii) $K'(H^+)_i$ change to 0.46 ± 0.01 μM, $p < 0.05$. (*p* values are in comparison with basal activity.)

As an example of the changes in the mutants compared with wild type NHE3, Y501A/R503A/K505A, which does not bind $PI(4,5)P_2$ or $PI(3,4,5)P_3$, had the following: (i) lower basal activity (basal activity V_{max}, 297 ± 45 $\mu M/s$, and $K'(H^+)_i$, 0.70 ± 0.11 μM), and (ii) no change in activity when exposed to serum or wortmannin (serum V_{max}, 310 ± 25 $\mu M/s$, NS, $K'(H^+)_i$, 0.68 ± 0.06 μM, NS, and wortmannin V_{max}, 360 ± 61 $\mu M/s$, NS, $K'(H^+)_i$, 0.72 ± 0.03 μM, NS) (Fig. 5, *B* and *H*, Table 1, and supplemental Table 1). The meaning of changes in basal transport is commented on under "Discussion."

As the bioinformatic analysis from Scansite predicted, Phe^{509} and two positive charges in the same amino acid cluster were important for phosphoinositide binding. As shown in Fig. 4, mutant F509A/R511A/R512A lost $PI(3,4,5)P_3$ and $PI(4,5)P_2$ binding. This mutant displayed lower serum stimulation ($55 \pm 2.6\%$), which was significantly different from WT serum stimulation ($75 \pm 4.3\%$ $p < 0.05$). In addition, this mutation had a wortmannin inhibitory response (68% inhibition $\pm 1.9\%$), which was significantly increased compared with WT wortmannin response ($50 \pm 5.4\%$, $p < 0.01$). Basal V_{max}, 452 ± 60 $\mu M/s$, serum V_{max}, 701 ± 12 $\mu M/s$, $p < 0.05$, wortmannin V_{max}, 145 ± 14 $\mu M/s$, $p < 0.05$, $K'(H^+)_i$ basal, 0.37 ± 0.07 μM, $K'(H^+)_i$ serum 0.29 ± 0.03 μM, NS; $K'(H^+)_i$ wortmannin, 0.62 ± 0.02 μM, $p < 0.05$ (Fig. 5, *C* and *H*, Table 1, and supplemental Table 1).

FIGURE 4. **Mutagenesis of positively charged amino acids in N-terminal part of cytosolic region of NHE3 alters $PI(3,4,5)P_3$ and $PI(4,5)P_2$ binding.** *A,* $PI(3,4,5)P_3$ and $PI(4,5)P_2$ liposomal pulldown assays were performed with 150 ng of WT F1 His$_6$ fusion protein and point mutated fusion proteins as follows: Y501A/R503A/K505A, R511L/R512L, F509A/R511A/R512A, and R551L/R552L as described in Fig. 1*A* and Table 1. Y501A/R503A/K505A, F509A/R511A/R512A, and R551L/R552L do not bind to $PI(4,5)P_2$ or $PI(3,4,5)P_3$ containing liposomes, whereas R511L/R512L had increased binding to $PI(4,5)P_2$ and $PI(3,4,5)P_3$. 150 ng of NHE3 fusion proteins were loaded as shown in the *lower panel*. *B,* $PI(3,4,5)P_3$ and $PI(4,5)P_2$ liposomal pulldown assays were performed with 150 ng of WT F1 His$_6$ fusion protein and point mutated fusion protein R520F/R527F. This mutant displayed greater reduction of $PI(3,4,5)P_3$ binding than $PI(4,5)P_2$ binding when compared with its control (68% loss *versus* 23%). Loading of 150 ng of proteins is shown in the *right-most lanes*. *C,* $PI(3,4,5)P_3$ and $PI(4,5)P_2$ liposomal pulldown assays were performed with 150 ng of WT F1 His$_6$ fusion protein and combination mutations Y501A/R503A/K505A + F509A/R511A/R512A. The combination mutation binds minimally with $PI(3,4,5)P_3$- and $PI(4,5)P_2$-containing liposomes. *D,* quantification: integrated intensity of bands from *A–C* was measured by Odyssey system (LI-COR). Pulldowns were done three times, and average values of integrated intensity were plotted as means ± S.E. Standard error is too small to see in Y501A/R503A/K505A and R520F/R527F $PI(3,4,5)P_3$, although F509A/R511A/R512A and R551L/R552L had approximately zero intensity values.

Representative trace for transport study of WT NHE3 under basal, serum and wortmannin conditions (N = 8)

Representative trace for transport study of Y501A/R503A/K505A under basal, serum and wortmannin conditions (N=6)

Representative trace for transport study of F509A/R511A/R512A under basal, serum and wortmannin conditions (N=5)

Representative trace for transport study of R511L/R512L under basal, serum and wortmannin conditions (N=5)

Representative trace for transport study of R520F/R527F under basal, serum and wortmannin conditions (N = 6)

Representative trace for transport study of R551L/R552L under basal, serum and wortmannin conditions. (N=5)

Representative trace for transport study of Y501A/R503A/K505A+ F509A/R511A/R512A under basal, serum and wortmannin conditions (N=5)

To determine whether the effect of mutations Y501A/R503A/K505A and F509A/R511A/R512A acted on similar or different pathways, a combination of both mutations was expressed in PS120 cells. This combination double mutant compared with WT had lower basal activity (V_{max}, 277 ± 86 μM/s, and $K'(H^+)_i$, 0.49 ± 0.07 μM) and no change in activity when exposed to serum or wortmannin (serum V_{max}, 248 ± 28 μM/s, NS, $K'(H^+)_i$ 0.45 ± 0.11 μM, NS and wortmannin V_{max}, 199 ± 13 μM/s, NS, $K'(H^+)_i$, 0.41 ± 0.08 μM, NS). Thus, this combination mutation mimics Y501A/R503A/K505A by itself with no evidence of additivity of effects of the two mutants (Fig. 5, *G* and *H*, Table 1, and supplemental Table 1).

To examine the role of Phe[509] in the effect of the Phe[509]/Arg[511]/Arg[512] mutant, Arg[511] and Arg[512] were mutated without mutating Phe[509], creating mutant R511L/R512L. This mutation had an increase in binding to PI(3,4,5)P$_3$ and PI(4,5)P$_2$ (Fig. 4, *A* and *D*). This mutant also had the following: (i) reduced basal NHE3 activity; (ii) increased NHE3 activity when exposed acutely to serum. This increase was statistically significantly greater than that which occurred in the wild type NHE3 (basal V_{max}, 76 ± 9 μM/s, serum V_{max}, 198 ± 15 μM/s, $p < 0.05$); there was a 160 ± 12.7% increase in R511L/R512L compared with 75 ± 4.3% in WT, $p < 0.05$ ($K'(H^+)_i$ basal, 0.61 ± 0.06 μM, $K'(H^+)_i$ serum, 0.40 ± 0.05 μM, $p < 0.05$); and (iii) decrease in wortmannin inhibition (30 ± 3.2% compared with 50 ± 5.4% in WT, $p < 0.01$); wortmannin V_{max}, 53 ± 5 μM/s, $p < 0.05$, $K'(H^+)_i$, 0.87 ± 0.03 μM, NS). Thus, the increase in PI(3,4,5)P$_3$ and PI(4,5)P$_2$ binding of this mutant correlated with an increase in serum stimulation of NHE3 activity (Fig. 5, *D* and *H*, Table 1, supplemental Table 1).

R520F/R527F, a mutation which previously had been shown to decrease ezrin binding to NHE3 by 80% (21), had greater loss of PI(3,4,5)P$_3$ binding (68%) compared with PI(4,5)P$_2$ binding (23%) (Fig. 4*B*). The mutation also displayed no serum response (basal V_{max}, 396 ± 58 μM/s, serum V_{max}, 450 ± 87 μM/s, NS) and normal wortmannin response (50% ± 6.7% inhibition; wortmannin V_{max}, 199 ± 40 μM/s, $p < 0.05$; $K'(H^+)_i$ basal 0.59 ± 0.08 μM, $K'(H^+)_i$ serum, 0.60 ± 0.07 μM, NS and $K'(H^+)_i$ wortmannin, 0.69 ± 0.05, $p < 0.05$) (Fig. 5, *E* and *H*, Table 1, supplemental Table 1).

Mutant R551L/R552L displayed loss of both PI(3,4,5)P$_3$ and PI(4,5)P$_2$ binding (Fig. 4, *A* and *D*) and functionally had no serum effect (V_{max} basal, 263 ± 27 μM/s, serum V_{max}, 240 ± 56 μM/s, NS) and a wortmannin inhibitory effect similar to wild type (50% ± 5.9% inhibition) (wortmannin V_{max}, 130 ± 13 μM/s, $p < 0.05$, $K'(H^+)_i$ basal, 0.42 ± 0.05 μM, $K'(H^+)_i$ serum, 0.47 ± 0.06 μM, NS, $K'(H^+)_i$, wortmannin, 0.60 ± 0.06 μM, $p < 0.05$) (Fig. 5, *F* and *H*, Table 1, supplemental Table 1).

Basal Surface Expression of NHE3 and F1 Mutants Does Not Correlate with PI(4,5)P$_2$ and PI(3,4,5)P$_3$ Binding of NHE3—Because most regulation of NHE3 occurs by changes in regulated endocytosis or exocytosis and affects surface expression of NHE3 (15), surface expression of WT and NHE3 mutant was determined under basal conditions using cell surface biotinylation of subconfluent PS120 cells. The fraction of surface NHE3 was expressed as percent of total NHE3. The amount of protein expressed was normalized to wild type as shown in Table 1 and Fig. 6. Mutants Y501A/R503A/K505A, F509A/R511A/R512A, and Y501A/R503A/K505A + F509A/R511A/R512A had similar % surface NHE3 as compared with wild type NHE3 (5.1, 5.1, and 4.7% *versus* 6.3% in WT) (Fig. 5, *A, B, D,* and *G*), but all had reduced total expression. In contrast, mutant R511L/R512L had 1.3% surface expression (as shown in Fig. 5*C*) and also had decreased total expression. Mutant R520F/R527F had 1.9% surface expression. Mutant R551L/R55 2L also had reduced surface expression (2.8%). Both of the last two NHE3 mutants had near normal total expression of NHE3. Thus several patterns of surface and total expression were observed as shown in Table 1.

DISCUSSION

In this study, we demonstrate that the N-terminal part of the NHE3 C terminus is involved in regulation of basal and serum-stimulated NHE3 activity by interaction with the phosphoinositides PI(3,4,5)P$_3$ and/or PI(4,5)P$_2$. The part of NHE3 involved includes amino acids 475–552 and appears to be made up of two regions that resemble each other in effects on phosphoinositide binding and on NHE3 activity but demonstrate enough differences to make us hypothesize that they both bind phosphoinositides differently and exert different effects on NHE3 activity. These two regions (Tyr[501]–Arg[512] and Arg[520]–Arg[552]) are both made up of two separate clusters of at least two positively charged amino acids. The first region also contains bulky, hydrophobic amino acids which when mutated alter the effects of the region on phosphoinositide binding and regulation of NHE3 activity. Mutations of each of the two positively charged clusters that make up each of the two regions behave similarly in terms of effects on NHE3 activity and phosphoinositide binding, suggesting they are acting similarly as part of a single functional domain. In fact, for the most N-terminal region, the effects on phosphoinositide binding and NHE3 activity were nonadditive when a combination made up of both mutations was studied, further supporting effects via a common mechanism. Moreover, differences in the effects of the two regions on both lipid binding and NHE3 activity are strongly suggestive that NHE3 interacts with membrane lipids using its F1 domain by more than a single mechanism. The similarities in effects of the two regions are that when mutated they all reduce basal NHE3 activity, abolish or significantly reduce serum stimulation of NHE3 activity, while also reducing liposomal binding to PI(4,5)P$_2$ and PI(3,4,5)P$_3$. All four mutations of NHE3, which make up the two regions, carry out basal NHE3 activity similar to that of wild type when transport activity is normalized to the

FIGURE 5. **Na$^+$/H$^+$ exchange rates for WT and NHE3 F1 point mutants expressed in PS120 cells.** *A–G,* basal rates (■), stimulation by serum (10%) (★), and inhibition by wortmannin (▼) (100 nM) are shown as V_{max} (μM/s) and $K'(H^+)_i$ (μM) for representative experiments and means ± S.E. for the series of experiments shown in text. NHE3 mutants Y501A/R503A/K505A, R520F/R527F, and R551L/R552L and Y501A/R503A/K505A + F509A/R511A/R512A lost serum stimulation. F509A/R511A/R512A showed a decrease in serum stimulation. R511L/R512L showed increased serum stimulation. All experiments were done using mixed pairs and repeated five or more times (*N* shown in individual legends). *H* represents comparison of V_{max} values of WT and NHE3 point mutations under basal, serum, and wortmannin conditions as mean ± S.E. (*, $p < 0.05$; for each NHE3 cell type, comparison of Na$^+$/H$^+$ exchange rates was done between basal/serum and basal/wortmannin).
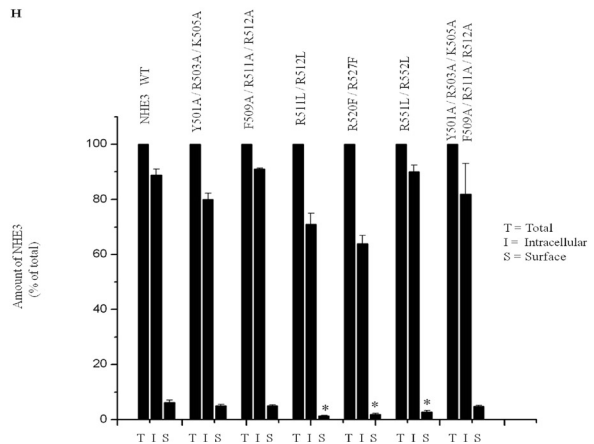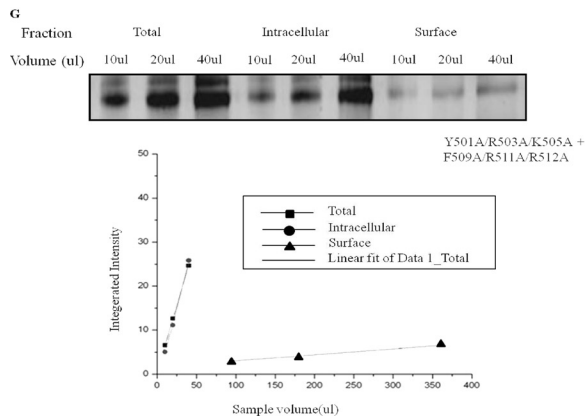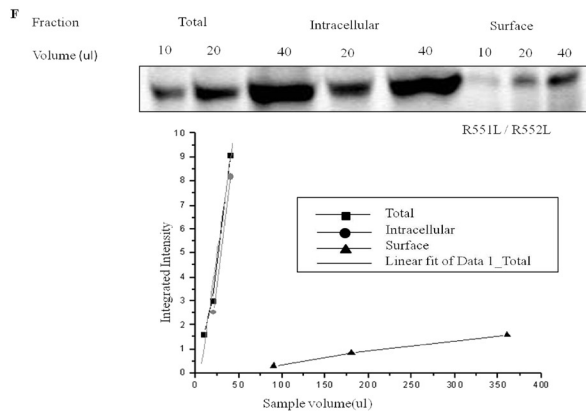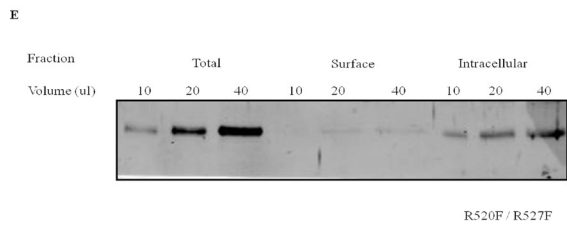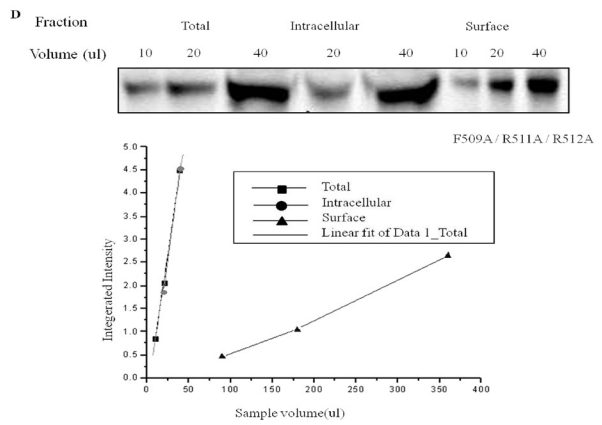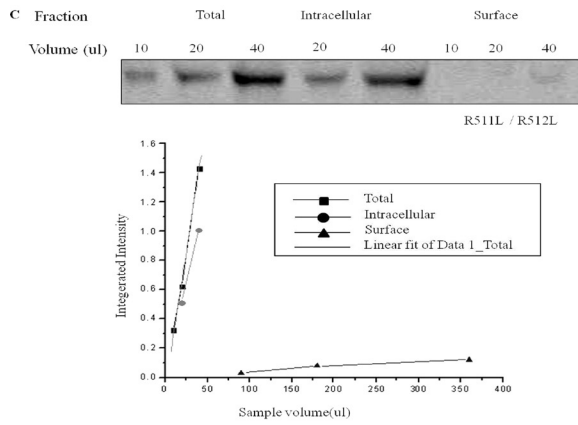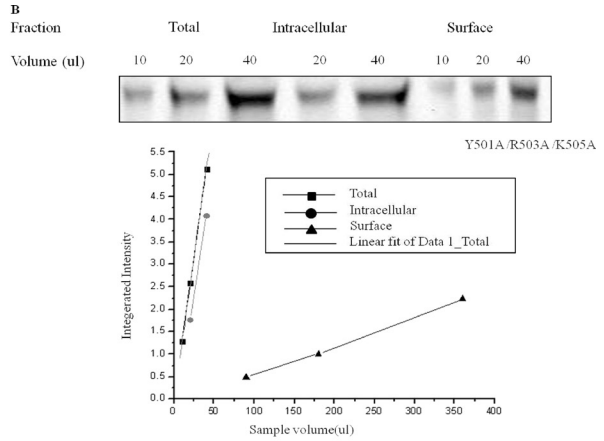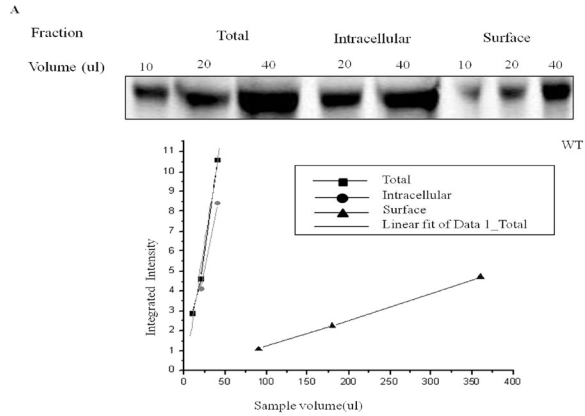
total number of NHE3 molecules estimated to be on the plasma membrane. In contrast, there are significant differences in the effects of the two regions. First, for the more N-terminal region, effects of mutating either of the two positively charged clusters similarly reduced binding of the NHE3 mutant to $PI(4,5)P_2$ and $PI(3,4,5)P_3$, and for the more C-terminal region, mutation of R520F/R527F reduced $PI(3,4,5)P_3$ binding more than $PI(4,5)P_2$ binding. This is the only suggestion from these studies that binding to $PI(3,4,5)P_3$ is more relevant for the effects of phosphoinositides on NHE3 activity than binding to $PI(4,5)P_2$. Second, mutations in all four positively charged clusters of amino acids (Y501A/R502A/K505A, F509A/R511A/R512A, R520F/R27F, and R551L/R552L) reduced the amount of plasma membrane NHE3. The more N-terminal mutations (Y501A/R502A/K505A and F509A/R511A/R512A) have reduced total NHE3 expression but similar percent plasma membrane expression compared with wild type; we have not examined the mechanism for this reduced total expression which is likely due to decreased synthesis or increased breakdown of mutant NHE3. The latter is known to occur with misfolded proteins as is well characterized for cystic fibrosis transmembrane regulator mutants (27). The more C-terminal (R520F/R527F and R551L/R552L) mutants have total NHE3 expression similar to wild type NHE3 but reduced percent plasma membrane expression compared with wild type. This indicates that the more C-terminal region but not the more N-terminal region alters NHE3 trafficking or plasma membrane retention. Of note in interpreting these differences is that Arg^{520}/Arg^{527} was previously shown to be in an α-helical domain in the NHE3 C terminus, which is where ezrin directly binds to the NHE3 C terminus and is necessary for multiple aspects of basal and regulated trafficking (21). Whether it is this direct ezrin binding or another property of this area of NHE3 that is responsible for the characteristics of this part of NHE3, including binding to phosphoinositides, is still an open question.

It is not surprising that phosphoinositide binding to NHE3 affected NHE3 activity. Detailed studies of rat NHE1 had previously shown that binding of $PI(4,5)P_2$ to amino acids 513–520 and 556–564 is necessary for basal Na^+/H^+ exchange activity (17). As shown in Fig. 1B, these regions of rat NHE1 are homologous to amino acids 465–472 and 509–516 of rabbit NHE3. The second of these motifs was shown in this study to be involved in $PI(4,5)P_2$ and $PI(3,4,5)P_3$ binding (*underlined* with a *brace* in Fig. 1A and as motif II in Fig. 1B), although the first homologous motif (motif I in Fig. 1B; corresponding to rabbit NHE3 amino acids 465–472) was not studied here because our

attempts to purify rabbit NHE3 N-terminal to amino acid 475 resulted in insoluble protein.

In addition, intracellular injection of $PI(3,4,5)P_3$ immediately stimulated NHE3 activity in opossum kidney cells, as reported by Fuster *et al.* (18). Our studies are a detailed mechanistic exploration of that finding. Our previous studies of NHE3 truncation mutations expressed in PS120 fibroblasts had demonstrated that regulation of NHE3 was dependent on different subdomains of the NHE3 C terminus (22, 28); stimulation of NHE3 by okadaic acid and FGF both occurred when NHE3 was truncated at amino acid 585 (22), consistent with the role for the F1 domain in maintaining basal NHE3 and serum stimulation as demonstrated in this study. Okadaic acid, which we showed acted on the NHE3 C terminus between amino acids 509 and 543 (22), has been shown also to be an activator of PI3K and Akt (29), suggesting that its role may involve phosphoinositide binding to, in addition to, or rather than by inhibition of phosphatases (PP1, PP2A, PP6, and PP4) (22, 30); however, the mechanism of okadaic acid stimulation of NHE3 remains controversial (30).

An unexpected finding was that mutating Arg^{511} and Arg^{512} in the N-terminal subdomain without altering Phe^{509} increased $PI(4,5)P_2$ and $PI(3,4,5)P_3$ binding, which was associated with an increase in the magnitude of the serum stimulation of this NHE3 mutant. Currently, we do not understand the mechanism for this increase in binding, and we speculate on a role for allosteric interactions leading to positive enhancement and/or alteration in intramolecular interactions between the positive amino acids Arg^{511}/Arg^{512} and negative amino acids such as Asp^{510}, which might lead to an alteration in the structural conformation of this region. However, this result strongly supports the involvement of phosphoinositide binding to this area of NHE3 in serum stimulation, because this mutant established a direct correlation between magnitude of serum stimulation of NHE3 activity and extent of NHE3 C-terminal binding to $PI(4,5)P_2/PI(3,4,5)P_3$, as shown in Table 1.

In previous studies of basal and acutely stimulated NHE3 activity in all cell culture models studied, ~50% of basal NHE3 activity was dependent on PI 3-kinase activity (15). Basal NHE3 activity was inhibited by exposure to the PI3K inhibitors, *viz.* LY594002 (31) and wortmannin (32, 33) at low doses, and acutely stimulated NHE3 was reduced by the same inhibitors between 50 and 100% based on the cell type expressing NHE3 and the ligand studied (FGF in PS120 cells by 50% (32); lysophosphatidic acid in opossum kidney cells by 100%) (31). These previous studies of PI3K dependence of basal and acutely stimulated NHE3 activity plus the rapid stimulation of NHE3 activity when $PI(3,4,5)_3$ was added to the

---

FIGURE 6. *A–H,* cell surface biotinylation studies show that surface expression of WT NHE3 and F1 domain positive cluster point mutations are not different and do not correlate with $PI(3,4,5)P_3$ and $PI(4,5)P_2$ binding. PS120 cells stable expressing WT HA-NHE3 and NHE3 point mutants were serum-starved for 5 h and then surface-biotinylated by NHS-SS-biotin. Representative Western blots for NHE3 and mutant proteins are shown, and means ± S.E. of surface expression are shown in *H* and Table 1. Multiple dilutions for total, intracellular (non-avidin-precipitated), and surface (avidin-precipitated) NHE3 were probed with anti-HA antibody. Protein density was measured by Odyssey Licor Biosystems, and densities were plotted against the sample volume (μl). Fractions were compared for analysis on a single Western blot. Percentage of NHE3 on surface was calculated by the product of dilution factor of surface and total NHE3 × ratio of surface NHE3 intensity/total NHE3 intensity. Surface biotinylation for WT (*A*) and the following mutants showed similar percentage surface expression: Y501A/R503A/K505A (*B* and *H*), F509A/R511A/R512A (*D* and *H*), and Y501A/R503A/K505A + F509A/R511A/R512A (*G* and *H*). In contrast, R511L/R512L (*C* and *H*), R520F/R527F (*E* and *H*), and R551L/R552L (*F* and *H*) had lower surface expression than wild type. *H* shows the amount of surface NHE3 as percentage of total NHE3, where total NHE3 was normalized to 100% for each condition; *p* value (*, *p* < 0.05) represents comparison of percent surface NHE3 for each mutant protein compared with wild type. Experiments were done three times for each mutant protein paired with a wild type NHE3, and data shown are means ± S.E.

inside of opossum kidney cells (18) suggest that $PI(3,4,5)P_3$ is the more relevant phosphoinositide for NHE3 regulation. However, this study does not separate the roles of $PI(4,5)P_2$ and $PI(3,4,5)P_3$, and either phosphoinositide could be relevant for physiologic or pathophysiologic regulation of NHE3. Importantly, this study did not show correlation of the extent of wortmannin inhibition of basal NHE3 activity with changes in phosphoinositide binding. This suggests that the domain of NHE3 involved in basal regulation by PI3K may be somewhat separate from the domains involved in serum-stimulated NHE3 activity. We do not rule out the possibility that mutagenesis of phosphoinositide-binding motifs can also alter association with interacting proteins in that area and contribute to alteration in NHE3 activity.

Many transport proteins have been shown to be regulated by phosphoinositides, with most emphasis being on interactions with $PI(4,5)P_2$ rather than $PI(3,4,5)P_3$. Recently, however, $PI(3,4,5)P_3$ was shown to regulate TRPC6 by disrupting its association with calmodulin (11), and $PI(4,5)P_2$ has been reported to be important for ENaC channel gating and $PI(3,4,5)P_3$ for ENaC channel open probability and number (9, 10). These results suggest that different phosphoinositides in a cell can regulate different functional aspects of the same protein. Understanding the mechanisms by which phosphoinositides contribute to basal and regulated activities of transporters, channels and pumps have lagged behind the description of their involvement. Two aspects of the phosphoinositide interacting domains have been identified in the regulated transporters. Heo *et al.* (34) demonstrated a role for positively charged amino acid clusters, which appear to be important for NHE3 effects. In contrast, multiple protein/lipid interacting domains have been identified by which proteins interact with lipids, some of which are used for phosphoinositide association. Sequence searches failed to identify specific lipid binding groups in the NHE3 C terminus. Nonetheless, the possibility of the presence of additional lipid binding groups in the NHE3 C terminus cannot be excluded, as experiments with a higher concentration of C-terminal peptides (300 ng) demonstrated weak binding of the NHE3 F2 region (amino acids 590–667) to $PI(3,4,5)P_3$ liposomes, although this binding was much less than that detected in the F1 region (supplemental Fig. 1). Thus, multiple low affinity or transiently interacting motifs capable of binding phosphoinositides might be present in the NHE3 C terminus.

In conclusion, NHE3 amino acids 475–589 bind phosphoinositides $PI(4,5)P_2$ and $PI(3,4,5)P_3$. Mutation of positively charged and hydrophobic amino acids in the NHE3 C-terminal F1 domain alters $PI(3,4,5)P_3$ and $PI(4,5)P_2$ binding. Thus phosphoinositide binding to NHE3 is dependent on charge-based interactions. Mutations that alter $PI(3,4,5)P_3$ and $PI(4,5)P_2$ binding of NHE3 all have decreased basal activity. Serum stimulation of NHE3 correlated with $PI(3,4,5)P_3$ and $PI(4,5)P_2$ binding of NHE3. In contrast, wortmannin inhibition of basal NHE3 activity did not correlate with $PI(3,4,5)P_3$ or $PI(4,5)P_2$ binding of NHE3. The NHE3 F1 domain (amino acids 475–589) has two distinct subdomains (Tyr^{501}–Arg^{512} and Arg^{520}–Arg^{552}), both of which are important for serum stimulation, but they display different effects in total and surface expression and phosphoinositide interactions. The close proximity of two different lipid binding groups suggests the possibility of their intermolecular interaction(s) under physiologic conditions in NHE3 regulation.

Recently, Wakabayashi *et al.* (35) identified a lipid binding domain in the intracellular C-terminal domain of NHE1, which incorporated the area previously shown to be the $PI(4,5)P_2$ binding domain. This domain of NHE1 physically associated with the plasma membrane under basal conditions and increased its binding with elevated diacylglycerol or phorbol ester exposure. Two subdomains in this area were tentatively identified, the N-terminal portion binding primarily to acidic phospholipids, and the C-terminal domain to diacylglycerol and phorbol esters. Shown in Fig. 1*B*, this domain of NHE1 overlaps almost totally with the homologous area of NHE3 we describe here, and we predict that these areas may behave similarly in terms of lipid binding and perhaps plasma membrane association. However, given that NHE1 is regulated primarily by changes in $K'(H^+)_i$ and NHE3 is regulated mostly by changes in trafficking, which include changes in V_{max} and to a lesser extent in $K'(H^+)_i$, indicate that these similar domains use different mechanisms for regulation of NHE1 and NHE3.

REFERENCES

1. Rosenhouse-Dantsker, A., and Logothetis, D. E. (2007) *Pflugers Arch.* **455,** 45–53
2. Hilgemann, D. W., and Ball, R. (1996) *Science* **273,** 956–959
3. Hilgemann, D. W., Feng, S., and Nasuhoglu, C. (2001) *Sci. STKE 2001,* re19
4. Logothetis, D. E., Petrou, V. I., Adney, S. K., and Mahajan, R. (2010) *Pflugers Arch.* **460,** 321–341
5. Rohacs, T. (2009) *Cell Calcium* **45,** 554–565
6. Gamper, N., and Shapiro, M. S. (2007) *Nat. Rev. Neurosci.* **8,** 921–934
7. Huang, C. L. (2007) *Am. J. Physiol. Renal Physiol.* **293,** F1761–F1765
8. Suh, B. C., and Hille, B. (2008) *Annu. Rev. Biophys.* **37,** 175–195
9. Pochynyuk, O., Bugaj, V., and Stockand, J. D. (2008) *Curr. Opin. Nephrol. Hypertens* **17,** 533–540
10. Pochynyuk, O., Tong, Q., Medina, J., Vandewalle, A., Staruschenko, A., Bugaj, V., and Stockand, J. D. (2007) *J. Gen. Physiol.* **130,** 399–413
11. Kwon, Y., Hofmann, T., and Montell, C. (2007) *Mol. Cell* **25,** 491–503
12. Rohács, T., Lopes, C. M., Michailidis, I., and Logothetis, D. E. (2005) *Nat. Neurosci.* **8,** 626–634
13. McLaughlin, S., and Murray, D. (2005) *Nature* **438,** 605–611
14. Falkenburger, B. H., Jensen, J. B., and Hille, B. (2010) *J. Gen. Physiol.* **135,** 99–114
15. Zachos, N. C., Tse, M., and Donowitz, M. (2005) *Annu. Rev. Physiol.* **67,** 411–443
16. Wakabayashi, S., Shigekawa, M., and Pouyssegur, J. (1997) *Physiol. Rev.* **77,** 51–74
17. Aharonovitz, O., Zaun, H. C., Balla, T., York, J. D., Orlowski, J., and Grinstein, S. (2000) *J. Cell Biol.* **150,** 213–224
18. Fuster, D., Moe, O. W., and Hilgemann, D. W. (2004) *Proc. Natl. Acad. Sci. U.S.A.* **101,** 10482–10487
19. Collins, M. O. (2009) *Science* **325,** 1635–1636
20. Murtazina, R., Kovbasnjuk, O., Donowitz, M., and Li, X. (2006) *J. Biol. Chem.* **281,** 17845–17855
21. Cha, B., Tse, M., Yun, C., Kovbasnjuk, O., Mohan, S., Hubbard, A., Arpin, M., and Donowitz, M. (2006) *Mol. Biol. Cell* **17,** 2661–2673
22. Levine, S. A., Nath, S. K., Yun, C. H., Yip, J. W., Montrose, M., Donowitz, M., and Tse, C. M. (1995) *J. Biol. Chem.* **270,** 13716–13725
23. Sarker, R., Grønborg, M., Cha, B., Mohan, S., Chen, Y., Pandey, A., Litchfield, D., Donowitz, M., and Li, X. (2008) *Mol. Biol. Cell* **19,** 3859–3870
24. Donowitz, M., Mohan, S., Zhu, C. X., Chen, T. E., Lin, R., Cha, B., Zachos,

N. C., Murtazina, R., Sarker, R., and Li, X. (2009) *J. Exp. Biol.* **212,** 1638–1646

25. Landau, M., Herz, K., Padan, E., and Ben-Tal, N. (2007) *J. Biol. Chem.* **282,** 37854–37863

26. Cha, B., Oh, S., Shanmugaratnam, J., Donowitz, M., and Yun, C. C. (2003) *J. Membr. Biol.* **191,** 49–58

27. Gelman, M. S., and Kopito, R. R. (2003) *Methods Mol. Biol.* **232,** 27–37

28. Akhter, S., Cavet, M. E., Tse, C. M., and Donowitz, M. (2000) *Biochemistry* **39,** 1990–2000

29. Atkinson, T., Whitfield, J., and Chakravarthy, B. (2009) *Biochem. Biophys. Res. Commun.* **378,** 394–398

30. Dynia, D. W., Steinmetz, A. G., and Kocinsky, H. S. (2010) *Am. J. Physiol. Renal Physiol* **298,** F745–F753

31. Lee-Kwon, W., Kawano, K., Choi, J. W., Kim, J. H., and Donowitz, M. (2003) *J. Biol. Chem.* **278,** 16494–16501

32. Janecki, A. J., Janecki, M., Akhter, S., and Donowitz, M. (2000) *J. Biol. Chem.* **275,** 8133–8142

33. Akhter, S., Kovbasnjuk, O., Li, X., Cavet, M., Noel, J., Arpin, M., Hubbard, A. L., and Donowitz, M. (2002) *Am. J. Physiol. Cell Physiol* **283,** C927–C940

34. Heo, W. D., Inoue, T., Park, W. S., Kim, M. L., Park, B. O., Wandless, T. J., and Meyer, T. (2006) *Science* **314,** 1458–1461

35. Wakabayashi, S., Nakamura, T. Y., Kobayashi, S., and Hisamitsu, T. (2010) *J. Biol. Chem.* **285,** 26652–26661